Available online at www.sciencedirect.com
SCIENCE DIRECT®
Chemical Physics Letters 387 (2004) 23–28
CHEMICAL PHYSICS LETTERS
www.elsevier.com/locate/cplett

Eu^{3+} doped yttrium oxysulfide nanocrystals – crystallite size and luminescence transition(s)

J. Dhanaraj [a], M. Geethalakshmi [b], R. Jagannathan [a,*], T.R.N. Kutty [c]

[a] *Materials Science Division, CECRI, Karaikudi 630 006, India*
[b] *Department of Materials Science, Madurai Kamaraj University, Madurai 625 021, India*
[c] *Materials Research Center, Indian Institute of Science, Bangalore 560 012, India*

Received 9 September 2003; in final form 9 December 2003
Published online: 21 February 2004

Abstract

Nanocrystals of yttrium oxysulfide doped with trivalent europium has been synthesized using a two step sol–gel polymer thermolysis method employing urea formaldehyde resin in the presence of ethylene diamine tetra acetic acid as chelating agent. In this synthesis, marginal tunability in crystallite size ($\phi = 7$–15 nm) was achieved by varying the concentration of reactants and organic precursors. In this nanocrystalline system, various luminescence transitions, in particular $^5D_0 \rightarrow {}^7F_2$ transition of Eu^{3+} shows moderate ($\sim 60\%$) lifetime shortening which can be explained by considering possible increase in non-radiative rate (τ_{nr}) and also possible modification in optical electronegativity induced by surface states of the crystallites.

1. Introduction

Quantum dot related structures constitute an interesting branch of materials science for investigation both from fundamental and applications points of view [1,2]. Trivalent europium doped yttrium oxysulfide is an important cathodoluminescent phosphor system finding applications in color television picture tubes and cathode ray tubes [3,4] and of late in field emission display devices [5]. Recently we succeeded [6] in synthesizing nanocrystalline Y_2O_2S:Eu^{3+} with an average crystallite size of $\Phi \sim 20$ nm using a gel-polymer thermolysis method [7] involving urea–formaldehyde resin (UFR). It would be interesting to see, if any quantum-dot like structure of this luminescence system having a bandgap of 4.8 eV grouped under large bandgap semiconductor [8] can be synthesized. With this objective, we propose a two-step sol–gel polymer method for synthesizing oxysulfide nanoparticles of still lower size (~10 nm) as schematized in Fig. 1.

2. Experimental aspects

2.1. Synthesis of Y_2O_2S:Eu^{3+} nanoparticles

In the two-step method employed for the synthesis of Y_2O_2S:Eu^{3+} nanocrystals, first step involves combustion synthesis of Y_2O_3:Eu^{3+} nanocrystals using urea–formaldehyde resin followed by sulfurization process leading to the formation of Y_2O_2S:Eu^{3+} nanocrystals. Well dispersed oxysulfide nanocrystals could be synthesized using the sol–gel polymer thermolysis method employing UFR as fuel cum dispersion matrix, sodium thiosulfate as sulfurizing agent and ethylene diamine tetra acetic acid (EDTA) as chelating agent for the formation of UFR resin.

First mixed Y/Eu$(NO_3)_3$ solutions were prepared using suitable molar concentrations of $Y(NO_3)_3$ (2.0–9.0 mM) and $Eu(NO_3)_3$ (0.1–0.8 mM) and this mixture was polymerized by adding EDTA (1.2–9.7 mM) urea (0.033 M), and formaldehyde (5 μM). The polymerized solution was subsequently heated to evaporate off excess water and the solidified mass was heated at 500 °C for 2 h. The white fluffy mass (nanocrystalline Y_2O_3:Eu^{3+}) was then digested with sodium thiosulfate (0.02–2.4

* Corresponding author.
E-mail address: jaga57_99@yahoo.com (R. Jagannathan).

0009-2614/$ - see front matter © 2004 Elsevier B.V. All rights reserved.
doi:10.1016/j.cplett.2004.01.079

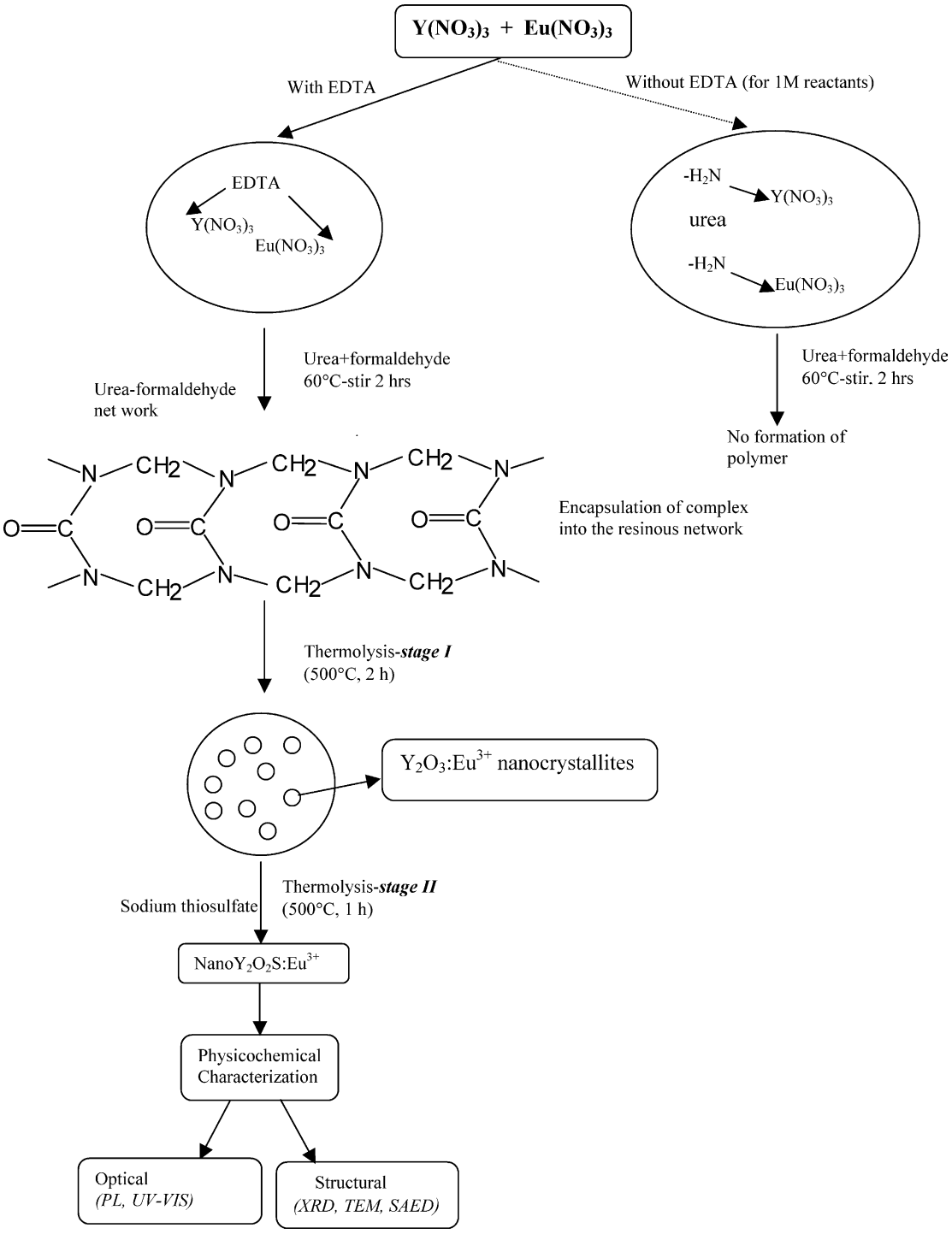

Fig. 1. Two stage synthesis for nanoparticles of $Y_2O_2S:Eu^{3+}$.

mM) on a hot plate until the water was completely evaporated off and the mixture was subsequently fired at 500 °C for 1 h resulting in nanocrystalline $Y_2O_2S:Eu^{3+}$. The synthesis is based on the premise that once nanoparticles of $Y_2O_3:Eu^{3+}$ are synthesized, subsequent sulfurization of the same would produce nanoparticles of $Y_2O_2S:Eu^{3+}$ retaining the morphology and size of the parent oxide crystallites. Particle size of the oxides can be varied by changing the concentration of the nitrate reactants (sol) dispersed in the resinous network. Also it should be noted that higher the concentration of reactants greater is the possibility of agglomeration and vice-versa.

The resin used in this investigation was prepared conventionally by the addition of urea and formaldehyde in the molar ratio 1:2 resulting in a condensation

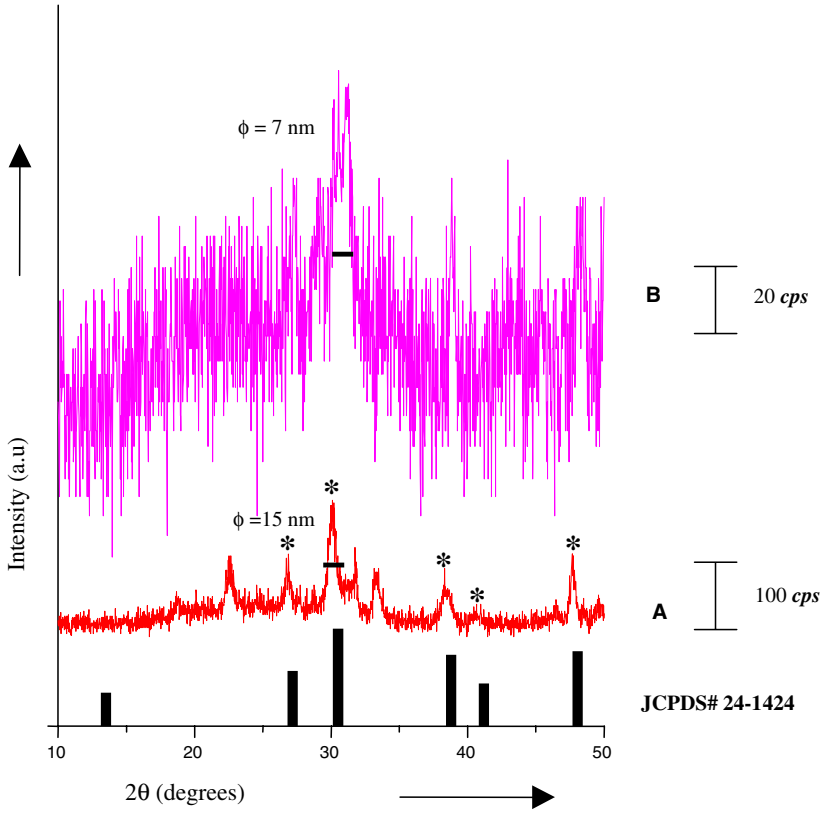

Fig. 2. XRD patterns of the nanocrystalline $Y_2O_2S:Eu^{3+}$ (1%) samples A and B. The particle size (ϕ) of the nano samples calculated using Scherrer formula are also indicated (* indicates Y_2O_2S phase).

reaction of urea and formaldehyde. Importantly during the course of the synthesis, in order to avoid formation of lanthanide complexes which otherwise would impede the formation of polymeric/resinous network, sufficient quantity of EDTA should be added [9]. Presence of transition/lanthanide metal ions can impede the gel-polymerization process [10] and also we observed that gel formation in presence of Y^{3+} and Eu^{3+} ions was difficult. This may be due to possible formation of Y/Eu-amino complexes hindering the gel formation. Hence use of a chelating agent such as EDTA may be useful. It has indeed been observed that addition of small quantities of EDTA was much useful to make the gel-formation easier. The amount of fuel and organic precursors to be added was calculated in relation to metallic/lanthanide nitrates in accordance with oxidizing/reducing valencies [11].

2.2. Characterization of $Y_2O_2S:Eu^{3+}$ nanoparticles

Unwashed samples as prepared without any further surface-treatment were used for X-ray powder diffraction (XRD) and photoluminescence studies. All measurements were made in the first few hours of sample preparation as described before [6,7]. Luminescence spectra and lifetime measurements presented in this study were made using Varian Cary-Eclipse fluorescence spectrophotometer equipped with Xe-arc flash lamp and grating with groove-density of 1200 lines/mm. Chemical purity of different samples synthesized was cross-checked using XRD technique and is consistent with Y_2O_2S phase (Fig. 2). There were traces of sodium polysulfide(s) as flux residues and its presence may not influence the luminescence properties. The crystallite-size estimated using XRD line-width data in conjunction with Scherrer formula [12] is also indicated in each case. In this report we discuss results corresponding to two nanocrystalline $Y_2O_2S:Eu^{3+}$ (1%) samples labeled as A and B having crystallite size (Φ) of 15 and 7 nm, respectively, in relation to bulk $Y_2O_2S:Eu^{3+}$ (1%) sample with a mean particle size of 1.5 μm. Tristimulus color coordinate values of bulk and nanocrystalline samples were determined using Minolta x–y 100 chromometer.

3. Results and discussion

3.1. Oxysulfide nanocrystals-size and morphology

In sol–gel synthesis of nanoceramics, gel formation providing basic network for the growth of crystallites and morphology is very crucial. Gel formation using organic polymeric precursors can lead to complex topology such as loops, branches and interconnections.

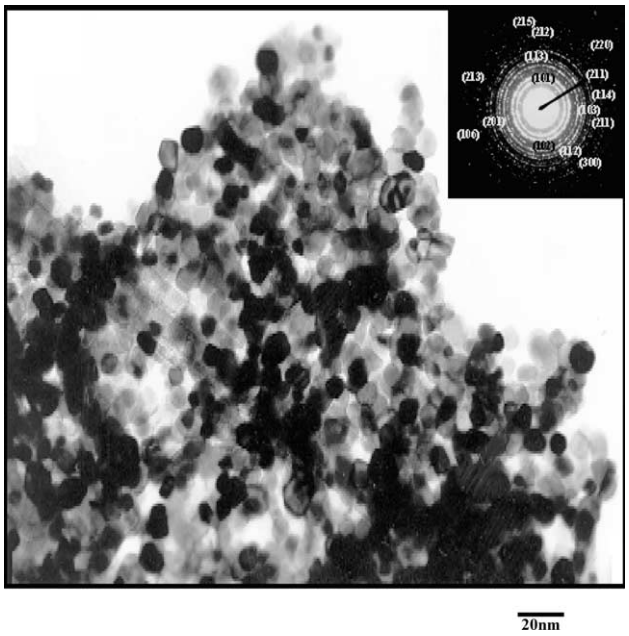

Fig. 3. Transmission electron microscope image of nanocrystalline $Y_2O_2S:Eu^{3+}$ sample (sample A). Inset: corresponding SAED pattern.

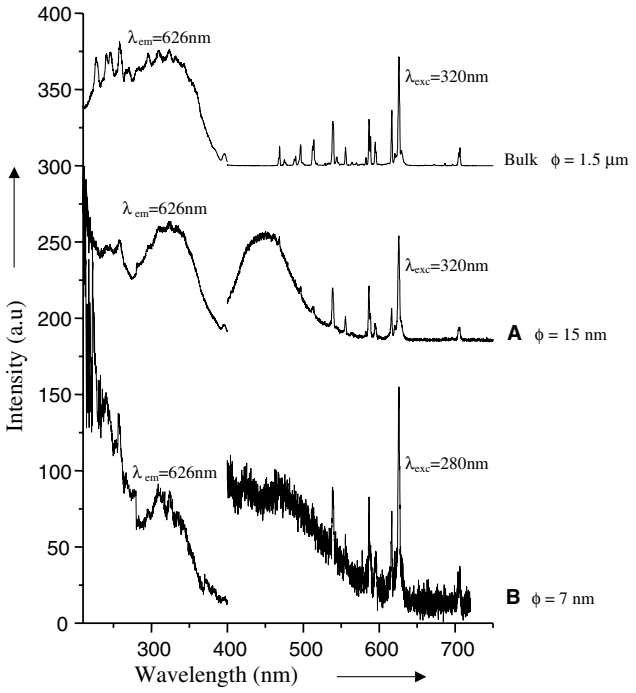

Fig. 4. Photoluminescence emission and excitation spectra ($T = 300$ K) of bulk and nanocrystalline $Y_2O_2S:Eu^{3+}$ (1%) samples. Corresponding emission and excitation wavelengths are indicated.

Upon thermolysis and sufurization, this leads to the formation of well dispersed $Y_2O_2S:Eu^{3+}$ nanoparticles having polyhedral/spherical morphology. Fig. 3 shows transmission electron microscope image of the thus prepared oxysulfide nanocrystals. Corresponding selected area electron diffraction pattern given in the inset of the figure is consistent with yttrium oxysulfide phase. Furthermore from Fig. 3 and Table 1 it should be noted that in this synthesis, some marginal size-tunability could be achieved. In particular lower crystallite size can be achieved by decreasing the concentration of the reactants and organic precursors.

3.2. Crystallite size and luminescence transitions of Eu^{3+} in Y_2O_2S nanocrystals

Intraconfigurational f–f type electronic transitions originating from trivalent europium doped yttrium oxysulfide nanocrystals seem to have profound dependence on the particle size. Upon photo-excitation, Eu^{3+} doped system shows-up wealth of Stark energy levels in the visible region. In particular, luminescence transitions corresponding to the $^5D_0 \rightarrow {}^7F_J$ manifold in the orange–red region are of practical significance. Eu^{3+} ion doped in Y_2O_2S matrix shows intense red emission around 626 nm due to $^5D_0 \rightarrow {}^7F_2$ transition working by electric dipole transition mechanism. This transition is known to be hypersensitive to crystal-structure and chemical surroundings [13]. Whereas the line emission observed in the orange region ($\sim$ 586 nm) due to $^5D_0 \rightarrow {}^7F_1$ transition working by magnetic dipole transition mechanism is insensitive to crystal-structure and chemical surroundings. On this consideration, this transition can be used as an internal standard to have some insights on transition strengths of various luminescence transitions of Eu^{3+} doped in a matrix [14]. Relative intensity of the hypersensitive transition with respect to the magnetic dipole transition as internal standard would give an idea on the transition strength of the hypersensitive transition. This seems to have profound dependence on the crystallite-size. In any case, if there is any change in the relative

Table 1
Crystallite size luminescence transitions of Eu^{3+} in nanocrystalline Y_2O_2S

Sample	Particle size	R.I $^5D_0 \rightarrow {}^7F_2$ / $^5D_0 \rightarrow {}^7F_1$	Color coordinates		$\tau(^5D_0 \rightarrow {}^7F_1)$		$\tau(^5D_0 \rightarrow {}^7F_2)$		$\tau(^5D_0 \rightarrow {}^7F_4)$	
			x	y	τ (ms)	Δ (%)	τ (ms)	Δ (%)	τ (ms)	Δ (%)
Bulk	1.5 μm	2.54	0.662	0.328	0.157	–	0.675	–	0.586	–
A	15 nm	1.802	0.357	0.270	0.157	0	0.652	−3.4	0.518	−6.8
B	7 nm	2.051	0.486	0.338	0.123	−21.7	0.276	−59.1	0.258	−56

'–' indicates decrease in lifetime (%) with respect to the bulk system.

intensities of Eu^{3+} transitions, this may be reflected in tri-stimulus color coordinates of this nanocrystalline system as listed in Table 1. These can arise from several reasons. The dominance of band emission observed in the blue region ($\lambda_{em} = 450$ nm) upon decreasing crystallite size can be ascribed to Y_2O_2S host-emission coupled with defect centers and surface states. This in turn can lead to decrease in red-color coordinate (x) (Table 1).

From Table 1, it can be seen that for 7 nm particles (sample B) there is marginal decrease (about 20%) in the observed luminescence lifetime for $^5D_0 \rightarrow {}^7F_1$ transition. On the other hand for the case of $^5D_0 \rightarrow {}^7F_2$ ($^7F_4$) transition, there is substantial decrease (over 50%) in the observed luminescence lifetimes in relation to that of the bulk sample. It should be noted that as the crystallite-size decreases from 15 to 7 nm there is nearly three fold decrease in fluorescence lifetimes of $^5D_0 \rightarrow {}^7F_2$ ($^7F_4$) transitions of Eu^{3+} (Table 1). Also for $^5D_0 \rightarrow {}^7F_4$ transition similar pronounced decrease in fluorescence lifetime was observed. Decrease in fluorescence lifetime observed would mean increase either in radiative transition or non-radiative transition rates or both. Using lifetime data (Fig. 5) it can be calculated that the total transition probability of the hypersensitive transition to be about 150 s^{-1} for the bulk Y_2O_2S:Eu^{3+} system while it increases to about 360 s^{-1} for sample B (size $\sim$ 7 nm).

From photoluminescence emission spectra it is not possible to conclude any obvious enhancement in the fluorescence emission intensity for Eu^{3+} luminescence transitions. On the otherhand, it seems possible that observed lifetime shortening may be due to increased non-radiative rate(s). The increase in non-radiative rates may be rationalized in terms of pronounced phonon-losses, non-radiative energy losses through channels related to defect-centers arising from surface states of the nanocrystals. Furthermore pronounced defect-centers is exemplified from the dominance of blue emission around 450 nm which may come from Y_2O_2S host having origin related to deep lying levels [15]. Dominance of blue emission in the nanocrystals may probably explain the decrease observed in tri-stimulus color coordinate corresponding to the red region (x). The intriguing point is, why the decrease in lifetime observed for the hypersensitive transitions should be more pronounced which is about three fold higher than the normal $^5D_0 \rightarrow {}^7F_1$ transition? In order to explain more pronounced decrease in luminescence lifetime for the hypersensitive transitions observed, we should consider other possibilities too. This means that the observed fluorescence lifetime shortening can be explained by considering increase in radiative transition rate of the hypersensitive transitions as well. Hence it is reasonable that transition strength of some of the selected f–f transitions of Eu^{3+} may undergo some size–induced change in oscillator strength as discussed below.

We have that the oscillator strength (P) of a f–f transition is given [16,17] by

$$P = (4\pi mc/3\hbar)\bar{\chi}\bar{\nu}\sum \Omega_\lambda |\langle 4f^N\psi J||U^{(\lambda)}||4f^N\psi' J'\rangle|^2(2J+1)^{-1} \quad \lambda = 2,4,6, \tag{1}$$

where $\bar{\nu}$ is the transition energy, χ is the field correction, $|\langle 4f^N\psi J||U^{(\lambda)}||4f^N\psi' J'\rangle|$ is the reduced matrix elements of intra- configurational tensor operator $U^{(\lambda)}$.$\langle\psi J|$, $|\psi' J'\rangle$ are the initial and final states of the transition, respectively, the intensity parameters Ω_λ including hypersensitivity [18] of the electronic transition, in particular for $\lambda = 2$.

From the structural data, we have that in the bulk system Eu^{3+} ion occupies an acentric site having C_{3v} local symmetry [19]. We have that between bulk and nano Y_2O_2S samples there are no obvious difference either in the lattice or in the local symmetries. Also from the experimental results it is not possible to predict multiple sites such as bulk, surface-sites occupied by Eu^{3+} in the nanocrystalline Y_2O_2S. For these reasons, it is reasonable to conclude that structural considerations cannot explain the pronounced life-time shortening observed in the hypersensitive transition. Alternatively, it seems possible that intensity of the hypersensitive transition can have profound dependence on electronegativity, ligand orbital ionization which has been extensively studied [20]. It is obvious that change in optical electronegativity of Eu^{3+}-ligand complex should be reflected in the position

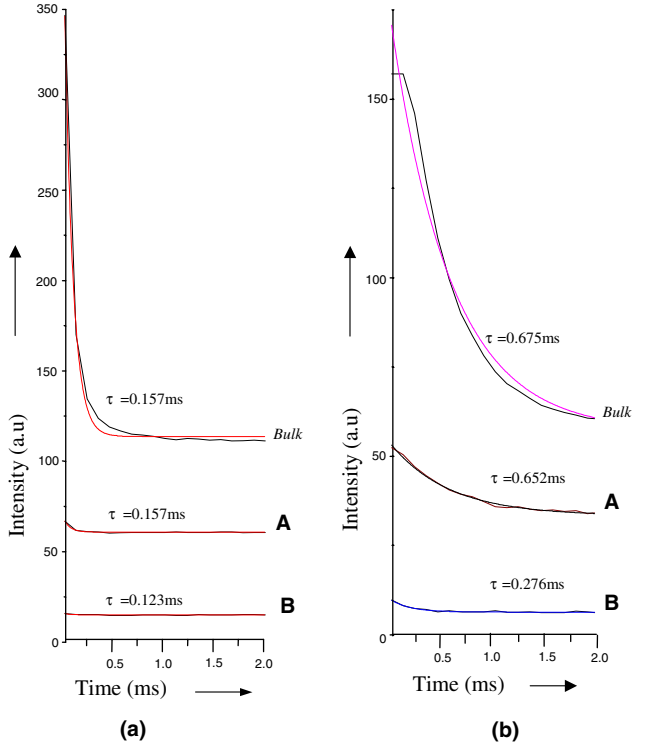

Fig. 5. (a) Fluorescence decay time profile for $^5D_0 \rightarrow {}^7F_1$ emission of Eu^{3+} in Y_2O_2S. (b) Fluorescence decay time profile for $^5D_0 \rightarrow {}^7F_2$ emission of Eu^{3+} in Y_2O_2S.

of the Eu^{3+}-ligand charge transfer excitation band. From Fig. 4, we observe that as the crystallite size decreases, there is red- shift in the excitation band corresponding to Eu^{3+}-ligand charge transfer transition. This implies a size dependent decrease in the optical electronegativity, which in turn may influence the intensity of the hypersensitive transition. Broken chemical bonds and lattice lacking long range periodicity can lead to the creation of surface states in the crystallites. This can influence electronegativity and polarisability of the Eu^{3+}-ligand complex in the crystallites. In particular Ω_2 parameter of the reduced matrix element U^{λ} shows critical dependence on covalency [21] and polarizability which in turn can determine the intensity of hypersensitive transition(s) of Eu^{3+} doped systems.

Extending the knowledge on intensity of hypersensitive transition(s) of lanthanide(s) in aqua-ion complexes derived using dynamic coupling mechanism [20], oscillator strength of the hyper-sensitive $^5D_0 \rightarrow {}^7F_2$ transition (P_{02}) can be given by

$$P_{02} = -1/3\langle \Delta\bar{\nu}\rangle[\bar{\alpha}(L)\langle\bar{\nu}\rangle(2J'+1)(4\pi^2 mc^2)] \quad (2)$$

with $\bar{\alpha}$ isotropic polarizability, $\Delta\bar{\nu}$ being the frequency shift in the hypersensitive transition that can be related to metal (Eu^{3+})-ligand covalency. The shift observed in Eu^{3+}-ligand charge transfer excitation band is the direct result of the modified metal-ligand covalency. This can be rationalized in terms of truncated chemical bonds leading to the formation of surface states which should be pronounced in the $Y_2O_2S{:}Eu^{3+}$ nanocrystalline wide-gap semiconductor system. Hence it is possible that change in optical electronegatitivity as a result of modification in Eu^{3+}-ligand covalency may influence the radiative transition rate of the hypersensitive transition. Furthermore, comparing excitation spectra of the present study with that in our earlier study [6] on $Y_2O_2S{:}Eu^{3+}$ nanocrystals synthesized using thermolysis of urea–formaldehyde resin, we observe that there is significant difference in the position and nature of shift in the excitation band. Preliminary study using FTIR spectra on these samples has indicated that chemisorbed species involved in these two cases are different which merits a detailed study. In any case, precise estimate of Judd–Ofelt parameters Ω_λ is necessary to confirm contribution from hypersensitivity of the Eu^{3+} transitions and this will be a part of our future goals of investigation on this nanocrystalline system. Hence at present the pronounced lifetime shortening observed for $^5D_0 \rightarrow {}^7F_2$ ($^7F_4$) hypersensitive transitions of Eu^{3+} in nanocrystalline Y_2O_2S remains as an open question.

4. Conclusions

In summary, trivalent europium doped yttrium oxysulfide nanocrystals with marginal size tunability (ϕ = 7–15 nm) was synthesized using a two-step sol–gel polymer thermolysis method. In this nanocrystalline system, luminescence transitions of Eu^{3+}, in particular, the hypersensitive $^5D_0 \rightarrow {}^7F_2$ ($^7F_4$) transitions show moderate lifetime shortening. This may possibly be attributed to increased non-radiative rate and modification in the Eu^{3+}-ligand covalency etc., necessitating further studies.

Acknowledgements

We thank the referees for the critical comments and helpful suggestions. We are grateful to the Department of Science & Technology, New Delhi for the financial support and J. Dhanaraj gratefully acknowledges Council of Scientific and Industrial Research for the award of a Senior Research Fellowship. Our tributes to Dr. Subbanna for TEM and sincere thanks to Dr. D.C. Trivedi and Ms. K.R. Sophya Preethi for the helps, encouragement we received in this work.

References

[1] P.A. Alivisatos, Science 271 (1996) 933.
[2] C.B. Murray, C.R. Kagan, M.G. Bawendi, Annu. Rev. Mater. Sci. 30 (2000) 545.
[3] M.R. Royce, U.S. Patent 3, 418, 246 (1968).
[4] M. Pham-Thi, A. Morell, J. Electrochem. Soc. 138 (1991) 1100.
[5] S.H. Cho, Y.S. Yoo, J.D. Lee, J. Electrochem. Soc. 145 (1998) 1017.
[6] J. Dhanaraj, R. Jagannathan, D.C. Trivedi, J. Mater. Chem. 13 (2003) 1778.
[7] J. Dhanaraj, R. Jagannathan, T.R.N. Kutty, C.H. Lu, J. Phys. Chem. B 1050 (2001) 11 098.
[8] M. Mikami, A. Oshiyama, Phys. Rev. B 57 (1998) 8939.
[9] F.J. Gotor, P. Odier, M. Gervais, J. Chosnet, P. Monod, Physica C 218 (1993) 429.
[10] A. Sin, P. Odier, Adv. Mater. 12 (2000) 649.
[11] S.R. Jain, K.C. Adiga, V.R. Pai Verneker, Combust. Flame. 40 (1981) 71.
[12] B.D. Cullity, Elements of X-ray diffraction, Addison-Wesley, Menlo Park, CA, 1956.
[13] G. Blasse, Struct. Bond. 26 (1976) 43.
[14] J.L. Adam, V. Poncon, J. Lucas, G. Boulon, J. Non-Cryst. Solids. 91 (1987) 191.
[15] M. Mikami, A. Oshiyama, Phys. Rev. B 60 (1999) 1707.
[16] B.R. Judd, Phys. Rev. 127 (1962) 750.
[17] G.S. Ofelt, J. Chem. Phys. 37 (1962) 511.
[18] W.T. Carnall, in: K.A. Gschneidner Jr., L. Eyring (Eds.), Handbook on the Physics and Chemistry of Rare Earths, North-Holland Publishing Company, 1979 (Chapter 24).
[19] B. Saubat, C. Fouassier, P. Hagenmuller, J. Bourcet, Mater. Res. Bull. 16 (1981) 193.
[20] S.F. Mason, R.D. Peacock, B. Stewart, Mole. Phys. 30 (1975) 1829.
[21] R. Reisfeld, C.K. Jorgensen, in: K.A. Gschneidner Jr., L. Eyring (Eds.), Handbook on the Physics and Chemistry of Rare Earths, North-Holland, Amsterdam, 1979 (Chapter 58).